UMYU Scientifica, Vol. 2 NO. 4, December 2023, Pp 136 – 144
https://doi.org/10.56919/usci.2324.017
ISSN: 2955 – 1145 (print); 2955 – 1153 (online)
A periodical of the Faculty of Natural and Applied Sciences, UMYU, Katsina

ORIGINAL RESEARCH ARTICLE

Adsorptive Removal of Phosphate from Agricultural Effluent using Thermally and Non-Thermally Activated Sepiolite Clay

Emmanuel Amuntse Yerima and Raymond Bwano Donatus.
Department of Chemical Sciences, Federal University Wukari, PMB 1020, Taraba State, Nigeria.

ABSTRACT

This study assessed the use of thermally activated sepiolite clay (TASC) and non-activated sepiolite clay (NASC) as adsorbents for phosphate adsorption from agricultural effluent. The effect of pH, temperature, dosage, and time on the adsorbates was investigated at pH 4-11, temperature 298 - 318k, contact time 30 – 120 minutes, and adsorbent dosage 0.2 - 4 g in 100 mL of agricultural effluent. Fourier-transformed infrared spectroscopy (FTIR) and Scanning electron microscope (SEM) techniques were used to determine adsorbent features. TASC and NASC exhibit an excellent capacity for adsorbing phosphate molecules. At equilibrium, the removal efficiency of phosphate at 4 different varying conditions of temperature, pH, adsorbent dosage, and time gave more than 100 % for TASC, while NASC also recorded over 100% adsorption of phosphate at 3 different varying conditions. The amount of phosphate adsorbed was found to decrease with an increase in temperature and contact time. The isotherm adsorption data fitted the Langmuir better than the Freundlich model, where the correlation coefficients of Langmuir and Freundlich were 0.9994 and 0.8901, respectively. The adsorption kinetics was better explained by the pseudo-first-order kinetic model with R^2 values TASC (0.9999) and NASC (0.9999) than the second order with R^2 value TASC (0.9984) and NASC (0.9820).

ARTICLE HISTORY

Received August 21, 2023.
Accepted November 28, 2023.
Published December 30, 2023.

KEYWORDS

Sepiolite, phosphate, adsorption and removal efficiency

INTRODUCTION

Intensive farming involving the application of substances, such as mineral fertilizers and chemical plant protection agents, has made it possible to obtain consistently high yields of agricultural plants to meet the population's food needs. However, several studies have shown that applying large amounts of mineral fertilizers can produce excessive phosphate, nitrates, and other nutrient levels in receiving water (Kumar *et al.,* 2019). Phosphorus is one of the essential nutrients necessary for the nutrition and growth of living organisms. Like nitrogen, it is a limiting nutrient for algal growth because it occurs in the least amount relative to the needs of plants. Phosphate is a vital nutrient for plant growth and, thus, responsible for a serious environmental problem termed eutrophication (Bandpi *et al.*, 2013; Yerima et al., 2022). Phosphate is among the most common anthropogenic groundwater pollutants, entering the human body through drinking water and vegetable products. Systematic human consumption of water and vegetables with excessive phosphate content may be associated with adverse health effects on humans, such as hyperphosphatemia and kidney and bone disorders.

Excessive phosphate in wastewater exists as orthophosphate, polyphosphate, and organically bound phosphate (Usman et al., 2022). Previous studies reveal that phosphates in wastewater have been removed using techniques such as ion exchange (Bektas et al., 2021) and chemical precipitation (Rajanjemi et al., 2021). However, both techniques suffer a setback due to the high cost and difficulty of operating at a low concentration of phosphates. Hence, the need to explore an adsorptive technique that allows for the reuse of adsorbent by activation has been considered more economical (Usman et al., 2022).

This research aims to assess the adsorptive removal of phosphate from agricultural effluent using sepiolite clay, an opaque, off-white, grey, or creamy-colored compound of hydrous magnesium silicate ($Mg_4Si6O_{15}(OH)_2{\cdot}6H_2O$), also known as petrosepiolitic (Francis *et al.*, 2014). This will help address problems associated with untreated, excessive phosphate in wastewater discharged into bigger water bodies, such as eutrophication (Lin et al., 2021), algae bloom leading to blockage of turbines and decline in

Correspondence: Emmanuel Amuntse Yerima. Department of Chemical Sciences, Federal University Wukari, PMB 1020, Taraba State, Nigeria. ✉ yerimaemmanuel@yahoo.com.
How to cite: Yerima, E. A., & Donatus, R. B. (2023). Adsorptive Removal of Phosphate from Agricultural Effluent using Thermally and Non-Thermally Activated Sepiolite Clay. *UMYU Scientifica*, 2(4), 136 – 144. https://doi.org/10.56919/usci.2324.017

water oxygen level and its effect on aquatic lives (Almanassra et al., 2021).

Sepiolite is useful as absorbents, environmental deodorants, catalyst carriers, and polyester asphalt coatings. It is renowned industrially for its water-holding and sorptive capacities (Andrejkovicova *et al.,* 2011). It has been reported that sepiolite-based materials can be used to remove a wide range of pollutant elements from water and soils (Wang et al., 2018). Despite its wide applications in various industrial processes, it has relatively low surface acidity, narrow channels, low surface area, and poor thermal stability. However, modification can enhance its sorption capacity (Jia *et al.,* 2011; Duan et al., 2013).

The experimental design and optimum condition for the adsorptive removal of phosphate by sepiolite was achieved by means of response surface methodology (RSM). The technique optimizes the response(s) when two or more quantitative factors are involved. The dependent variables are known as responses, and the independent variables or factors are primarily the predictor variables in response surface methodology (Karmoker *et al*., 2019).

MATERIALS AND METHODS

Sample collection

The sepiolite clay (adsorbent) used in this work was delivered by Central Drug House (P) Ltd. 7/28 Vardaan, Daryaganj, New Delhi-110002 (INDIA). Agricultural effluent samples were collected at five coordinates using well-labeled pre-clean plastic bottles (750 mL). The agricultural effluents were collected by random sampling at Rafin-Kada, Wukari, an agrarian settlement in Nigeria on the coordinate 7° and 43' N and 9° 53' E with a population size of about 241,546 based on the 2006 census and are predominantly farmers (Oko *et al.,* 2017; Yerima *et al.,* 2022). The Samples were immediately homogenized in ice coolers packed with ice before being transported to the laboratory for onward adsorption experiment at varying pH, temperature, adsorbent dosage, and contact time (Shigut *et al.,* 2017).

Table 1: Location and coordinates of sampling site

Sample	Point coordinate	Location
Sample A	7°706418N, 9°891373E	Rafinkada
Sample B	7°706750N, 9°891606E	Rafinkada
Sample C	7°706748N, 9°891362E	Rafinkada
Sample D	7°706674N, 9°890679E	Rafinkada
Sample E	7°706858N, 9°891258E	Rafinkada

Sample preparation and conditioning

Thermally activated sepiolite clay was obtained by weighing 166.62 g of raw sepiolite clay and calcined in a muffle furnace at 600°C for 1 hr. It was then cooled, sealed in an air-tight container, and labeled as TASC, while the raw sepiolite was tagged as non-activated sepiolite clay (NASC).

The experimental design was carried out with the aid of "Design Expert software version 13," which suggested twenty-five experimental run times at varying temperatures (25 - 45°C), varying dosages of sepiolite clay (0.2 - 4g), varying pH (4 - 11) and varying contact time (30 - 120 minutes).

As the design expert software recommended, varying amounts of TASC (0.2 – 4g) were weighed into 25 different 100 mL of agricultural effluents. Drop-wise addition of 0.1 M NaOH and 0.1 M HCl was used to adjust the pH of the solution with the aid of a pH meter until the desired pH (4 - 11), varying temperature (25 - 45°C), and The solutions were stirred at varying contact time (30 – 120 minutes) with the aid of mechanical shaker and a water bath respectively until equilibrium was achieved and filtrate obtained. The same process was carried out on NASC. The concentration of the phosphate was determined before and after the batch adsorption process

Characterization of sepiolite clay

The Scanning Electronic Microscope (Model JOEL JSM 7600F) operated with an argon atmosphere using a current of 6 mA for 3 min to examine the morphology of TASC and NASC. The Fourier Transform Infrared (FT-IR) (Model Nicolet iS10 FT-IR Spectrometer) determined the functional groups with all spectra recorded from 4000 to 400 cm^{-1}.

Determination of phosphate

The phosphate concentration before adsorptive removal and the residual concentration after adsorption were analyzed using a 721D UV/VIS spectrophotometer. This was done by adding 5 mL of the sample into a 25 mL volumetric flask; 5 mL of the molybdate reagent and 1 mL of tin chloride working solution were added to it respectively and diluted to 25 mL with distilled water. The absorbance was taken using a UV/VIS spectrophotometer at wavelength 660nm. The phosphate concentration in the samples was calculated using the regression values from the calibration curve:

$y = 0.0004x + 0.0635$, $R^2 = 0.9952$ (Nagul *et al.,* 2015).

Data Analyses

The adsorption capacity (q_e) and adsorptive removal efficiency (R_e) were calculated using the concentration difference between the initial and equilibrium concentrations in equations 1 and 2. Co = initial concentration of ammonium, Ce = equilibrium concentration of ammonium, M = mass of adsorbent (ball clay), V = solution volume, and Re = adsorptive removal efficiency (Seliem et al., 2023).

Adsorption capacity (q_e) = $\frac{C_o - C_e}{M} \times V$ (1)

Removal efficiency (R_e) = $\frac{C_o - C_e}{C_o} \times 100$ (2)

To evaluate the adsorption kinetics of ammonium, the pseudo-first order kinetic model and pseudo-second-order kinetic model were employed, as shown in equations 3 and 4 where K_1 and K_2 are constants of the equilibrium rate (Ngouateu et al., 2015; Egah et al., 2019).

Pseudo-first order kinetic model: $\log(q_m - q_t) = \log q_m - \frac{k_1}{2.303} t$ (3)

Second-order kinetic model: $\frac{t}{q_t} = \frac{1}{k_2 q_m^2} + \frac{1}{q_m} t$ (4)

Where K_1 and q_m can be obtained from the plot of $\log(q_m - q_t)$ Versus (t) which gives $\frac{k_1}{2.303}$ as slope and $\log q_e$ As intercept for the pseudo-first order kinetic model, similarly, for the pseudo-second-order, the kinetic constant k_2 and the theoretical q_m can be calculated from the plots of $(\frac{t}{q_t})$ versus (t).

To further analyze the adsorption mechanism, the Langmuir and Freundlich isotherm models were adopted (Egah et al., 2019).

Langmuir: $\frac{C_e}{q_e} = \frac{1}{K_2 q_o} + \frac{C_e}{q_o}$ (5)

A plot between C_e/q_e versus C_e will generate a straight line with a slope of $1/q_o$ and an intercept equal to $1/k_2 q_o$.

Freundlich: $\ln q_e = \ln b + \frac{1}{n} \ln C_e$ (6)

A plot of $\ln q_e$ versus $\ln C_e$ produces a straight line with a slope= 1/n and intercept = ln b.

RESULTS AND DISCUSSION

The surface morphology of TASC and NASC analyzed using a scanning electron microscope (SEM - JEOL, JSM 7600 F) showed the presence of good porosity that will aid the interaction between the phosphate molecules and the adsorbents. Figure 1 revealed that TASC and NASC have similar characters at 8000 and 10000 magnification, respectively. The micrograph shows the presence of compact tubular crystals and mono-disperse particle size on the surface, which increases the surface active site of the adsorbent for adsorption (Ahmed *et al.*, 2015). However, the porosity was more prominent in NASC compared to TASC as displayed at 10000 magnification; this agrees with reports of effected temperature on the surface morphology of sepiolite (Feng *et al.*, 2007; Wang et al., 2018).

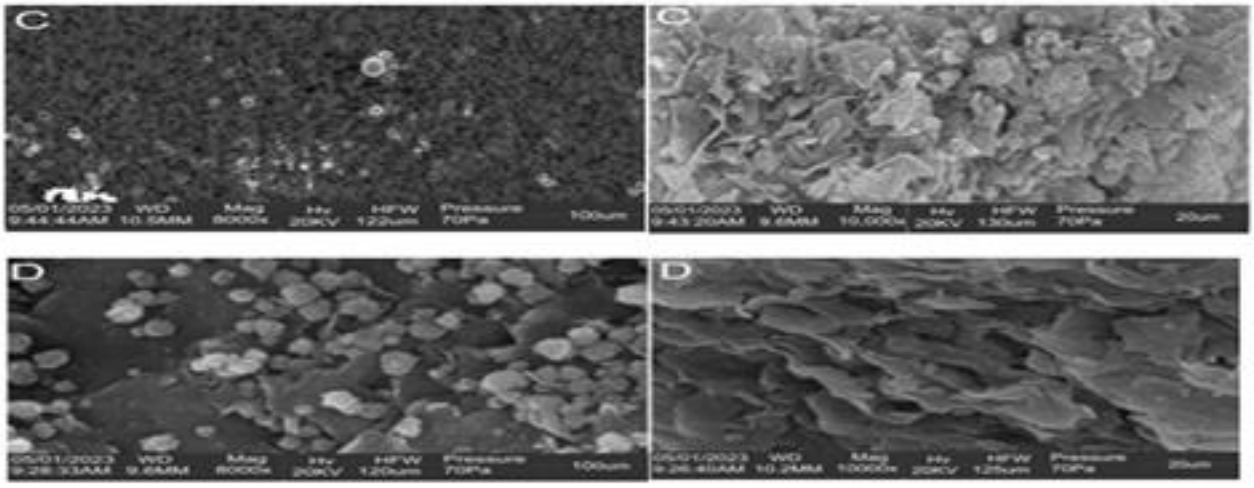

Figure 1: Scanning Electronic Microscope TASC (C) and NASC (D) at 8,000 and 10000 magnification

The FTIR spectrum in Figures 2 and 3 is important in identifying surface functional groups, which greatly influence adsorption. Good adsorbents have specific properties such as large pores, oxygen availability, hydrogen content, and Hydroxyl group (Kibami *et al.*, 2014). The FT-IR spectrum of TASC and NASC reveals broadband within the frequency range of (3000-4000 cm^{-1}), synonymous with O-H stretching vibrations (Mohammad *et al.*, 2010). The bands at 1650 – 1580 cm^{-1} are attributed to the N-H bending vibration of an amine, while peaks within 1415-1380 cm^{-1} imply S=O stretching in sulfate and sulfoxide then peaks within 1200 – 1000 cm^{-1} is for Si-O-Si stretching vibration mode (Borrajo et al., 2004), the band within 920 – 905 implies O-H bending in carboxylic acid (Faye and Fernandez, 2014). The 730 – 665 cm-1 peaks suggest C-H bending of alkynes, while the 600-500 cm-1 peak implies C-Br stretching in halo compounds (Moradi *et al.*, 2015). Other bands found in the spectrum of NASC within 850 – 550 cm^{-1} are synonymous with alkyl halide.

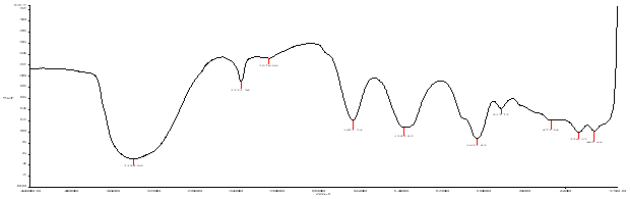

Figure 2: FT-IR Spectrum for Thermally Activated Sepiolite clay (TASC)

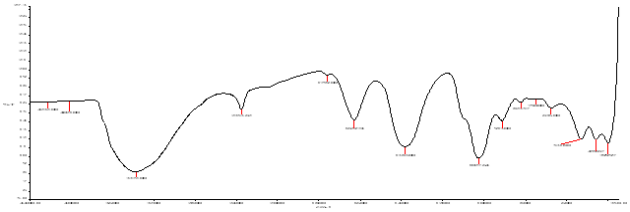

Figure 3: FT-IR Spectrum for Non-Activated Sepiolite Clay (NASC)

Batch Adsorption Experiments

The Design Expert version 13" recommends 25 experimental runs for phosphate removal in agricultural effluent within varying conditions: temperature (25 - 45°C), a dosage of ball clay adsorbent (0.5g - 4g), varying pH (3 - 11) and contact time (30 - 120 minutes) with the corresponding residual phosphate content after adsorptive removal as demonstrated in Table 2.

The optimum condition for the adsorptive removal of phosphate in the effluent by TASC was achieved at a temperature of 45°C, a dosage of 0.2 g, a pH of 7.5, and a contact time of 75 minutes with removal efficiencies of 133.3 % while by NABC was achieved at a temperature of 25°C, a dosage of 0.2 g, pH of 7.5 and contact time of 75 minutes with removal efficiencies of 121%. This is better than the 90.02% phosphate removal in waste by calcined cockle shells at 0.1 dosage (Kasim et al., 2020) as well as the 79% maximum phosphate adsorption on leftover coal obtained at a contact time of 200 min, an initial phosphate concentration of 5 mg/L, and a solution pH of 2.3 (Mekonnen et al., 2020).

The adsorption removal efficiency of phosphate by TASC and NASC was over 100% at 4 and 3 conditions, respectively. The removal efficiencies were much more than the 48% and 79 % removal efficiency of phosphate reported using kaolin–sodium bentonite and kaolin-organic bentonite respectively, under the condition of temperature 25°C adsorption time 360 minutes and pH 9.1 (Ren *et al.,* 2013).

Effect of pH on adsorption of phosphate

Figure 4 shows the mean amount of phosphate adsorbed increases from 35 mg/L to 40 mg/L with the corresponding increase in pH from 4 to 7.5, respectively. However, as the pH increases to 11, the amount adsorbed decreases to 32.5 mg/L for NASC. A similar trend was observed when TASC was used as an absorbent, giving an optimum removal of phosphate at the pH of 7.5, possibly due to an increase in electrostatic attraction between the adsorbate and adsorbents (Bolat *et al.,* 2010). Results showed that at a pH of 7.5, phosphates dissociate into phosphorus and hydroxide ions, which were then adsorbed by the positively charged adsorbent surfaces. However, as the pH approached alkaline at 11, there was a decrease due to repulsion between the adsorbate – adsorbent surface, as the negative charges decreased (Denizli *et al.,* 2001).

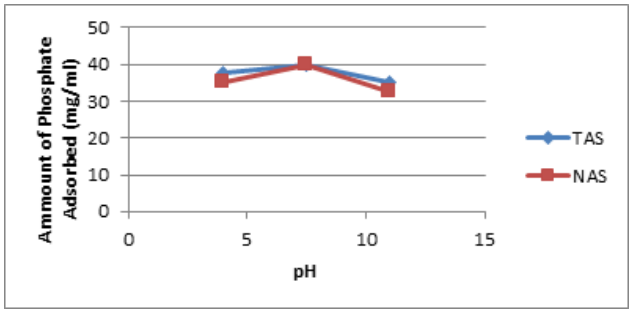

Figure 4: Effect of pH on Adsorption of Phosphate

Effect of adsorbent dosage on phosphate adsorption

The effect of adsorbent dosage of TASC and NASC on the removal of phosphate demonstrated in Figure 5 revealed a mean increase in percentage removal from 37.43 mg/L to 40.0 mg/L when TASC and NASC were increased from 0.2 g to 4.0 g respectively. The increase may be due to increased surface charges that favor sorbent-solute interactions (Mohammad *et al.*, 2010) and large surface area for phosphate adsorption (Nanganoa *et al.,* 2014).

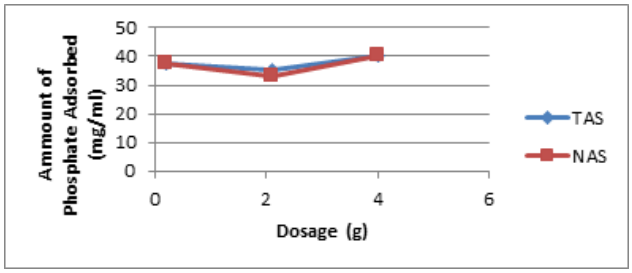

Figure 5 Effect of Adsorbent Dosage on Adsorption of Phosphate

3.3 Effect of temperature on phosphate adsorption

The effect of temperature on the adsorption of phosphate showed that as the temperature increases from 298K - 318K, the mean removal of phosphate decreases and sets as initial for TASC while for NASC decreases from 40g to 35.25 g respectively displayed in Figure 6. This agrees with the assertion that temperature affects the surface morphology of sepiolite and sorption capacity (Feng *et al.,* 2007; Wang et al., 2018).

Table 2: Phosphate residual concentrations and adsorption removal efficiency

Run	Tempt (°C)	Dosage (g)	pH	Time (mins)	TASC Res. Conc. PO_4^{3-} (mg/mL)	Qe (mg/L)	Re (%)	NASC. Res. Conc. of PO_4^{3-} (mg/mL)	Qe (mg/L)	Re (%)
1	35	0.2	4	75	6.25	17.5	84.85	18.75	11.25	54.54
2	25	2.1	4	75	6.25	1.67	84.85	6.25	1.67	84.84
3	25	2.1	11	75	33.75	0.357	18.18+	36.25	0.24	12.12
4	35	0.2	7.5	120	3.75	18.75	90.90	16.25	12.5	60.60
5	25	2.1	7.5	30	8.75	1.55	78.78	21.25	0.95	48.48
6	35	2.1	11	120	13.75	1.31	66.66	11.25	1.43	72.72
7	25	0.2	7.5	75	16.25	12.5	60.60	-8.75	20.6	121*
8	45	2.1	7.5	120	13.75	1.31	66.66	33.75	0.36	18.18
9	35	4	7.5	30	1.25	1	96.97	8.75	0.81	78.78
10	35	2.1	4	120	6.25	1.67	84.85	21.25	0.95	48.48
11	35	0.2	7.5	30	-8.75	20.6	121	11.25	15	72.72
12	45	2.1	11	75	6.25	1.67	84.84	36.25	0.24	12.12
13	35	4	7.5	120	11.25	0.75	72.72	28.75	0.31	30.30
14	45	4	7.5	75	8.75	0.81	78.78	-1.25	1.03	103
15	45	2.1	4	75	21.25	0.95	48.48	26.25	0.714	36.36
16	35	4	4	75	3.75	0.13	90.90	1.25	1	96.96
17	35	4	11	75	36.25	0.13	12.12	18.75	0.563	54.54
18	45	2.1	7.5	30	18.75	1.07	54.54	-6.25	1.96	115
19	35	2.1	4	30	6.25	1.67	84.84	28.75	0.595	30.30
20	35	2.1	11	30	-6.25	1.96	115	8.75	1.548	78.78
21	35	0.2	11	75	3.75	18.75	90.90	1.25	20	96.96
22	25	2.1	7.5	120	-6.25	1.96	115	1.25	1.904	96.96
23	35	2.1	7.5	75	18.75	1.07	54.54	36.25	0.238	12.12
24	45	0.2	7.5	75	-13.75	20.6	133.3*	6.25	17.5	84.84
25	25	4	7.5	75	33.75	0.19	18.18+	38.75	0.0625	6.06+
IC					41.25			41.25		

KEY: Re = adsorptive removal efficiency, Qe = adsorption capacity, * = Optimum adsorption, + = minimum adsorption, Res. Conc. = residual concentration, IC = residual concentration,

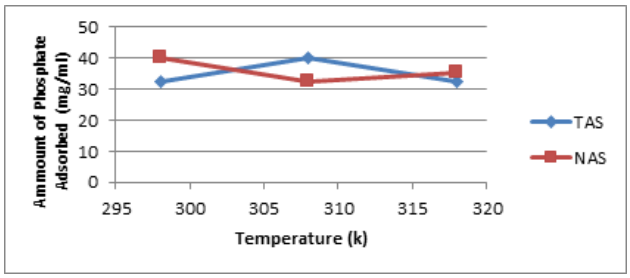

Figure 6 Effect of Temperature on Adsorption of Phosphate

Effect of contact time on phosphate adsorption

The effect of contact time on phosphate adsorption, shown in Figure 7, reveals a mean decreases from 40 to 35.25 mg/L and 40 to 32.5 mg/L for TASC and NASC, respectively, as contact increases from 30 – 120 minutes until equilibrium was attained at 120 minutes. The adsorption rate appeared quite high in the first 30 minutes, which could be explained by the high number of adsorption sites from the start (Ahmed *et al.*, 2015). As the time increased, the adsorption sites became gradually saturated until equilibrium was attained at 120 minutes (Riebe and Bunnenberg, 2007). This may be due to the ions' gradual saturation of the active sites as the contact time increases (Bhattacharyya and Gupta, 2011).

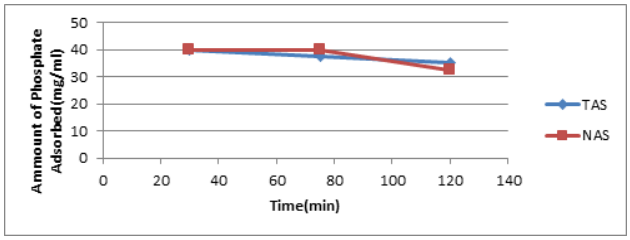

Figure 7: Effect of Contact Time on Adsorption of Phosphate

Adsorption Kinetic Model

Data obtained from the effect of contact time on phosphate adsorption were fitted into the kinetic models as shown in equations 3 and 4. The kinetic parameters in Table 3 showed that both first and second-order kinetic models could describe the phosphate adsorption on TASC and NASC. From their correlation coefficient R^2, it was observed that the Blanchard pseudo-first order gave better fittings with R^2 values ranging from 0.9999 - 0.9999 as compared with the Lagergren pseudo-second-order, which gave lower R^2 values ranging from 0.9820 - 0.9984 and the pseudo-first-order rate constant K_2 was in the range 0.0000167 - 0.000246 $g.mg^{-1}min^{-1}$. The high value of R^2 for the first–order shows that the pseudo-first-order best describes the whole adsorption process, indicating that physisorption is predominant on all adsorbents as the rate-determining step (Ajay *et al.*, 2015). This is in contrast with a recent study on the adsorption of phosphate, which shows that the pseudo-second-order kinetic model with an R^2 value of 0.99994 is higher than the pseudo-first-order with an R^2 value of 0.98391, which makes the pseudo-second-order more favorable than the first order (Ren *et al.*, 2013).

Table 3: Kinetic Parameters for Adsorption Lagergren First Order and Blanchard Second Order for Phosphate

Model	Parameter	TAS	NAS
First Order	K_1 (min^{-1})	0.0000167	0.000246
	Qe (mg/g)	0.5851	0.8232
	R^2	0.9999	0.9999
Second Order	K_2 (min^{-1})	0.000246	0.000273
	Qe (mg/g)	0.6839	0.4519
	R^2	0.9984	0.9820

KEY: TAS –Thermal Activated Sepiolite: NAS–Non-Activated Sepiolite

Adsorption Isotherm Models

The isotherm parameters obtained in this study and displayed in Table 4 reveal that both Langmuir and Freundlich isotherms can describe phosphate adsorption. However, the correlation coefficient R^2 of Langmuir isotherms (0.9994) was greater than that of Freundlich isotherms (0.8901). This suggests that the mechanism of phosphate adsorption is best explained by Langmuir isotherm. And can be concluded, based on this model, that the active sites on the adsorbent surface were homogeneously distributed and formed a monolayer adsorption (Bai *et al.*, 2010). The theoretical values of Langmuir constants Q_m and K_L were calculated from the slope and intercept of a linear plot of 1/Qe versus 1/Ce, respectively, revealing Qm values of 0.3975 mg/g and 0.3025 mg/g for TASC and NASC, respectively. The R_L values were found to be > 1 and > 0, indicating favorable adsorption for all adsorbents (Krishna and Swamy, 2012). However, the above mechanism for phosphate adsorption by sepiolite clay contradicts the removal by kaolin organic bentonite with a correlation coefficient of 0.945 in favor of Freundlich isotherm (Huang *et al.*, 2017).

Table 4: Isotherm Parameters for Phosphate Adsorption on Adsorbents

Model	Parameters	TAS	NAS
Langmuir Isotherm	Qm (mg/ml)	0.3975	0.3025
	K_L	0.0234	0.0242
	R^2	0.9994	0.9982
	R_L	1.036	0.080
Freundlich Isotherm	K_F	0.00153	0.00053
	R^2	0.8579	0.8901
	1/n	1.6356	0.7095
	n_F	0.6114	1.4094

KEY: TAS –Thermal Activated Sepiolite NAS–Non-Activated Sepiolite

CONCLUSION

Thermally activated sepiolite clay (TASC) and non-activated sepiolite clay (NASC) exhibited excellent physicochemical attributes of good adsorbents. And can serve as potent adsorbents for adsorbing phosphate from agricultural effluents with 100% adsorption efficiencies if given the right pH conditions, adsorbent dosage, temperature, and contact time, respectively. The mechanism of phosphate removal is best explained using the linearized Langmuir isotherm and the pseudo-first-order kinetic model. However, further studies can be conducted on alternative adsorbents to determine their urea removal efficiency.

REFERENCES

Ahmed, A. S, Tantawy, A. M. Abdallah, M. E. and Qassim, I. M. (2015). Characterization and Application of Kaolinite Clay as Solid Phase Extractor for Removal of Copper ions from Environmental Water Samples. International Journal of Advanced Research, 3 (3): 1-21.

Ajay, K. A. Mahendra, S. K. Chandrashekhar P. P, Ishwardas L. M. (2015). Kinetics Study on the Adsorption of Ni2+ ions onto Fly Ash. Journal of Chemical Technology and Metallurgy. 50 (5): 601- 609

Almanassra, I. W., Kochkodan, V., Mckay, G., Atieh, M. A. and Al-Ansari, T. (2021). Review of phosphate removal from water by carbonaceous sorbents. Journal of Environmental Management, 287, 12245. **[Crossref]**

Andrejkovičová, S. Ferraz, E. Velosa, A. L. Silva, A. S. Rocha, and F. (2011). "Fine Sepiolite Addition to Air Lime-metakaolin Mortars". Clay Minerals, 46 (4): 621- 635. **[Crossref]**

Bai, T. M, Komali. K. and Ventakeswarhi P. (2010). Equilibrium, Kinetics and Thermodynamic Studies on Biosorption of Copper and Zinc from Mixed Solution by Erythrina Variegata Orientalis Leaf Powder. India Journal of Chemical Technology, 17: 346 - 355.

Bandpi, David , and Zazouli, (2013). Biological Nitrate Removal Processes from Drinking Water Supply-A review. Journal of Environmental Health Science and Engineering, 11 (1): 35. **[Crossref]**

Bektaş T. E., Kıvanç Uğurluoğlu B. and Tan, B. (2021). Phosphate Removal by Ion Exchange in Batch Mode. Water Practice and Technology, 16: 1343 - 1354. **[Crossref]**

Bhattacharyya, K. G, and Gupta S. S, (2011). Removal of Cu (II) by Natural and Acid-activated Clays: An Insight of Adsorption Isotherm, Kinetics and Thermodynamics. Desalination, 272: 66-75. **[Crossref]**

Bolat F, Govori S, Haziri A, Spahiu S and Faiku F. (2010). "Used Tea Waste Adsorption for Removal of Phenol From Synthetic and Kosovo Industrial Waste-water". International Journal, Environmental Application and Science, 1: 63-67.

Borrajo, J.P., Liste, S., Serra, J., Gonzalez, P., Chiussi, S., Leon, B., Perez-Amor, M., Ylanen, H.O. and Hupa, M. (2004). Influence of the Network Modifier Content on the Bioactivity of Silicate

Glasses. Engineering Materials, 254 - 256 (1): 23 - 26. [Crossref]

Denizli A, Ozkan, G. and Ucar, M. (2001). Removal of Chlorophenols from Aquatic Systems with Dye Affinity Microbeads. Separation and Purification Technology, 24 (1-2): 255-62. [Crossref]

Duan, E., Han, J., Song, Y., Guan, Y., Zhao, W., Yang, B. and Guo, B. (2013). Adsorption of Styrene on Hydrothermal-modified Sepiolite. Material Letters, 111:150-153. [Crossref]

Egah, G.O., Hikon, B.N., Sheckhar, N.G. Yerima, E.A., Omovo, M., and Aminu, F.A. (2019). Synergistic Study of Hydroxyiron (III) and Kaolinite Composite for the Adsorptive Removal of Phenol and Cadmium. International Journal of Environmental Chemistry, 3(1): 30-42. [Crossref]

Faye, G. Bekele, W. and Fernandez, N. (2014). Removal of Nitrate ion from Aqueous Solution by Modified Ethiopian Bentonite Clay. International Journal of Research in Pharmacy and Chemistry, 4 (1): 192-201

Feng, Y. Master's Thesis. University of South; Hengyang, China. (2007). Study on the Adsorption of Lead and Cadmium by Sepiolite. Separation and Purification Technology, 24 (1-2): 255-62.

Francis, M. Louise, E., Freddie, V. Fey, M., Poch, R. M. (2014). Petroduric and Petrosepiolitic Horizons in Soils of Namaqualand, South Africa. Spanish Journal of Soil Science2: 142. hdl:10459.1/59295. ISSN 2253 - 6574. S2CID 220755679. [Crossref]

Huang , Z. Li ,Y., Chen W. Shi J. Zhang, N. Wang ,X. Li, Z. Gao, L. Zhang andY. (2017). Modified Bentonite Adsorption of Organic Pollutants of Dye Wastewater. Material Chemical Physics 202: 266 - 276. [Crossref]

Jia, M., Dai, Y., Du, T. and Liu, C. (2011). Preparation of Magnetically Modified Sepiolite and Adsorption of Hexavalent Chromium. Environmental Chemistry, 30:1546-1552

Karmoker, J.R. Hasan, I. Ahmed, N. Saifuddin, M. Reza, and M.S. (2019). "Development and Optimization of Acyclovir Loaded Mucoadhesive Microspheres by Box -Behnken Design".Dhaka University Journal of Pharmaceutical Sciences. 18 (1): 1- 12. [Crossref]

Kasim, N.Z., Malek, N.A.A., Anuwar, N.S.H., Hamid, N.H. (2020). Adsorptive removal of phosphate from aqueous solution using waste chicken bone and waste cockle shell. Materials Today: Proceedings, 31: 1. [Crossref]

Kibami, D. Pongener,C. Rao, K. S. and Sinha, D. (2014). Preparation and Characterization of Activated Carbon from Fagopyrum esculentum Moench by HNO3 and H3PO4 Chemical Activation. Der Chemica Sinica, 5 (4): 46-55.

Krishna, H. R. and Swamy S. V. V. (2012). A. Physico-Chemical Key Parameters, Langmuir and Freundlich Isotherm and Lagergren Rate Constant Studies on the Removal of Divalent Nickel from the Aqueous Solutions onto Powder of Calcined Brick. International Journal of Engineering Research and Development, 4 (1): 29-38.

Kumar, I. A. Jeyaprabha, C. M. and Viswanathan, S. N. (2019). Hydrothermal Encapsulation of Lanthanum Oxide Derived Aegle marmelos Admixed Chitosan Bead System for Nitrate and Phosphate Retention. International journal Biology macromolecule, 130: 527-535. [Crossref]

Lin, Q., Zhang, K., McGowan, S., Capo, C. and Shen, J. (2021). Synergistic impacts of nutrient enrichment and climate change on long-term water quality and ecological dynamics in contrasting shallow-lake zones. Limnology and Oceanography, 66, 3271–3286. [Crossref]

Mekonnen, D.T.; Alemayehu, E.; Lennartz, B. (2020). Removal of Phosphate Ions from Aqueous Solutions by Adsorption onto Leftover Coal. Water, 12: 1381. [Crossref]

Mohammad, W. A. Fawwaz, I. K. and Akl, A. M. (2010). Adsorption of Lead, Zinc and Cadmium Ions on Polyphosphate-modified Kaolinite Clay. Journal of Environmental Chemistry and Ecotoxicology. 2 (1): 001-008

Moradi, M. Dehpahlavan, A. Kalantary, R. R. Ameri, A. Farzadkia, M. and Izanoo, H. (2015). Application of Modified Bentonite using Sulfuric Acid for the Removal of Hexavalent Chromium from Aqueous Solutions. Environmental Health Engineering and Management Journal, 2 (3): 99-106.

Nagul, E. A. Mckelvie, I. D., Worsfold, P., Koslev, S.D. (2015). The Molybdenium Blue Reaction for the Determination of Phosphate Revisited. Opening the Black Box. Analytical chimica acta, 890: 60-82. [Crossref]

Nanganoa, L. T. Ketcha, J. M, and Ndi, J. N. (2014). Kinetic and Equilibrium Modeling of the

Adsorption of Amaranth from Aqueous Solution onto Smectite Clay. Research Journal of Chemical Sciences, 4 (2): 7-14.

Ngouateu, L. R. B., Sone, P.M.A., Nsami, N.J., Kouotou D., Belibi, P. D. and Mbadcam, K. J. (2015). Kinetics and Equilibrium Studies of the Adsorption of Phenol and Methylene Blue onto Cola Nutshell Based Activated Carbon. International Journal of Current Research Reviews, 7(9): 1-9.

Oko, J.A., Aremu, M.O. and Andrew, C. (2017). Evaluation of the Physicochemical and Heavy Metal Content of Ground Water Sources in Bantaji and Rafin-Kada settlements of Wukari Local Government Area, Taraba State, Nigeria. Journal of Environmental Chemistry and Ecotoxicology; 9(4): 43-53. **[Crossref]**

Rajaniemi, K., Hu, T., Nurmesniemi, E. T., Tuomikoski S. and Lassi, U. (2021). Phosphate and Ammonium Removal from Water through Electrochemical and Chemical Precipitation of Struvite. Processes, 9: 150. **[Crossref]**

Ren, N., Zhou, X., Guo, W. and Yang, S. (2013). A review on Treatment Methods of Dye Wastewater. CIESC Journal, 64: 84-94.

Riebe, B. and Bunnenberg, C. (2007). "Influence of Temperature Pre-Treatment and High-Molar Saline Solutions on the Adsorption Capacity of Organo-Clay Minerals", Physics and Chemistry of the Earth, 32: 581-587. **[Crossref]**

Seliem, M. K., Komarneni, S., Byrne T. et al. (2013). "Removal of Perchlorate by Synthetic Organosilicas and Organoclay: Kinetics and Isotherm Studies," Applied Clay Science, 71: 21-26. **[Crossref]**

Shigut, D.A. Liknew, G. Irge, D.D. and Ahmad, T. (2017). Assessment of Physico-chemical Quality of Borehole and Spring Water Sources Supplied to Robe Town, Oromia Region, Ethiopia. Applied Water Science, 7(1): 155-164. **[Crossref]**

Usman, M.O., Aturagaba, G., Ntale, M. And Nyakairu, G.W. (2022). A Review of Adsorption Techniques for Removal of Phosphates from Wastewater. Water Science Technology, (2022) 86 (12): 3113-3132. **[Crossref]**

Wang, Z.; Liao, L.; Hursthouse, A.; Song, N.; Ren, B.(2018). Sepiolite-Based Adsorbents for the Removal of Potentially Toxic Elements from Water: A Strategic Review for the Case of Environmental Contamination in Hunan, China. Int. J. Environ. Res. Public Health 15, 1653. **[Crossref]**

Yerima, E. A.; Kamba, E. A.; Egah, G. O.; Maaji, S. P.; Ibrahim, A. I. and Zulkifli, S. (2022). Evaluation of Quality Index of Borehole Water in Marmara and New Site Communities of Wukari, Nigeria. UMYU Scientifica, 1(1), 114 - 121. **[Crossref]**

Yerima, E.A., Itodo, A.U., Sha'Atob, R. and Wuana, R.A. (2022). Levels and Ecological Risk Assessment of Mineral and Heavy Metals in Soils Around Nasara Fertilizer Blending Plant, Lafia, Nigeria. Chemistry of the Total Environment, 2 (1): 1 - 9. **[Crossref]**.